Adding EUV reflectance to aluminum-coated mirrors for space-based observation

David D. Allred*, R. Steven Turley, Stephanie M. Thomas, Spencer G. Willett, Michael J. Greenburg, and Spencer B. Perry
Department of Physics and Astronomy, Brigham Young University, Provo, Utah, USA 84602

ABSTRACT

Protective layers on aluminum mirror surfaces which can be removed via the use of atomic hydrogen or hydrogen plasmas at the point of use in space may allow an expansion of broad-band mirrors into the EUV. LUVOIR (large, UV-optical-IR telescope) is a potential NASA flagship space-based observatory of the 2020's or 30's. It would utilize the largest mirrors ever flown[1]. Their reflective coating will almost certainly be aluminum, since such telescopes would profit from truly broad-band mirrors. To achieve reflectance over the broadest band, the top surface of such aluminum mirrors, however, needs to be bare, without the oxide layers that naturally form in air. This will open the 11 to 15 eV band. Since thin aluminum films are largely transparent between 15 and 70 eV an EUV mirror under the aluminum could make EUV bands such as 30.4 nm available for space-based astrophysics without sacrificing mirror IR, visible and UV reflectance. The local space environment for the observatory is sufficiently oxygen-free that the surface should remain bare for decades. We discuss protecting as-deposited aluminum mirrors with robust, oxygen-impenetrable, barrier layers applied in vacuo to the aluminum immediately after deposition and before air contact. The goal is that the barrier could also be cleanly, and relatively easily, removed once the mirror is in space. We propose hydrogen atoms as the means for removing the overcoat, since they can be expected to meet the criteria that the means is gentle enough to not roughen the mirror surface, and does not redeposit material on the mirror or other spacecraft components. We have investigated both organic and inorganic (such as, a-Si) hydrogen-removable films that can be applied to the aluminum immediately after its deposition have been investigated. We also examined the REVAP technique, using Cd and Zn. Agglomeration limited their effectiveness as barrier layers. That and dealing with the re-evaporated atoms may limit their utility as barrier materials.

Keywords: ultraviolet, extreme ultraviolet, mirrors, barrier layer, ellipsometry, hydrogen etch, genetic algorithm,

1. INTRODUCTION

It can be argued that the best IR-optical-UV-EUV broadband mirror for a space observatory that nature allows will be an EUV multilayer mirror coated by a very thin bare aluminum layer. We report early work along the path to using bare aluminum in space so that the effective bandwidth of UV-optical-IR, near normal-incidence mirror coatings can be expanded into the EUV either as 'extended mirrors' or 'dual-band' mirrors. The focus of this report is on issues related to coatings that can be removed in space.

Aluminum is the only material which can provide broad-band IR-optical-UV reflectance. Bare, first-surface aluminum can (theoretically) provide >85% reflectance up to 14 eV (>89 nm) and >90% over most of the 0-14 eV range. See Figure 1. (Reflectance in all figures are calculated from near-normal angle-of-incidence-unless noted otherwise – reflectance was computed using the Parrett equations and based on literature optical constants.) Unfortunately, aluminum will oxidize quickly when exposed to air. Even under high-vacuum conditions slow loss of vacuum ultraviolet (VUV) reflectance is observed[2]. The aluminum oxide which forms, though only 3.5-5nm thick, effectively blocks aluminum's high reflectance above ~9eV (<140 nm), which is the point at which sapphire's absorption constant rises above 0.01/nm[3].

To overcome this difficulty, wide-bandgap, metal fluoride thin films have been deposited on the aluminum film before it is exposed to air. Of these, lithium fluoride has the widest bandgap 13.6 eV (91.2nm). It is, however, hygroscopic and cannot, by itself, protect the aluminum for long periods of time. Magnesium fluoride, bandgap 10.8 eV (115nm) and, recently, aluminum fluoride (AlF_3) are often used in its place or as capping layers on LiF[4,5]. It also has been reported that depositing the films on a heated substrate and using a coating containing several layers allows the total

* allred@byu.edu; phone 1-801-422-3489; fax 1-801-422-0553

thicknesses of the fluoride layers to be decreased without sacrificing the barrier properties of the overcoats[4]. This allows the region of high reflectance to be expanded to slightly shorter wavelengths.

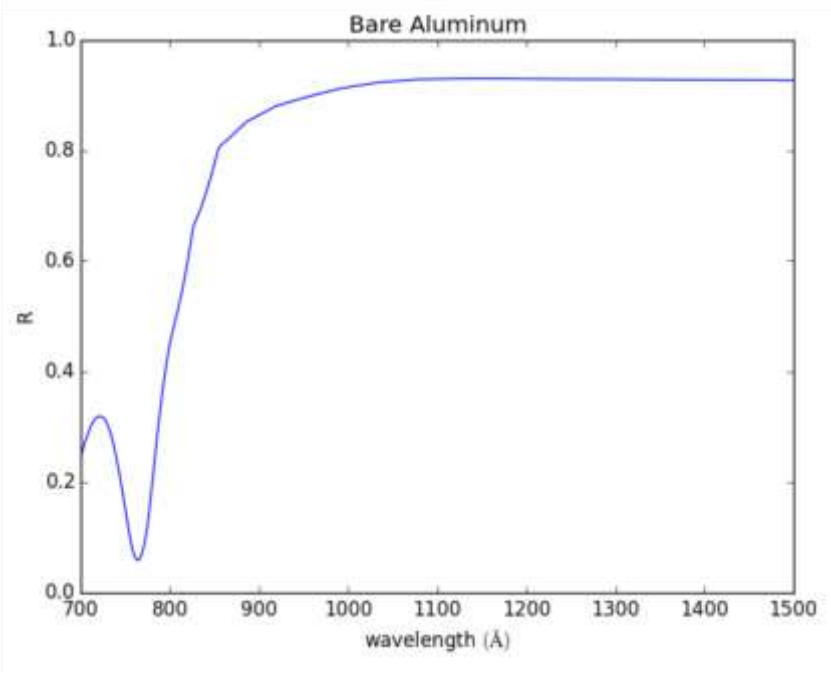


Figure 1. Computed normal-incidence reflectance of a bare Al thin film on SiC.

For some, the approach for achieving high reflectance at shorter wavelength without sacrificing barrier properties has been to explore alternate deposition techniques, such as atomic layer deposition (ALD)[6]. ALD is known to be capable of conformally coating some surfaces better than evaporation or sputtering processes. Again, the goal is to decrease the barrier thickness without giving up stability over the expected lifetime of the mirror[5-8]. There is a limit to how thin the fluoride overcoats can be made. Is there a path to improved performance beyond that?

The creation of broadband aluminum + EUV mirror options could support astrophysics of energetic sources, solar-system science and aspects of exoplanet characterization[9,10]. Scowen et al. have made a strong case that the astrophysics community needs space-based telescopes with far UV capability (at least to 90 nm)[11]. There are many summaries of the applications of the spectral lines that this would allow. See, for example, Scowen[11], Moore[6], and also see "Table 1: Significant Diagnostic Spectral Lines in the UV (50-250nm)" in Balasubramanian[5]. Some of the noteworthy lines are the more energetic hydrogen Lyman transitions (beta, gamma etc.), day-glow oxygen 83.4nm[12], and He I and He II lines[13]. While the opacity of the interstellar medium attenuates photons more energetic than 13.6 eV (91nm), as EUVE showed, there are important astrophysical phenomena to observe in the EUV[14]. Aluminum is 'transparent' down to the wavelength of 17.2nm (the band edge of aluminum L light). At this point the interstellar medium is a factor of a hundred more transparent than at 91nm[15]. Thus, there may be interstellar and intergalactic applications for EUV observations[16], especially if the observatory were to have orders of magnitude more light gathering than past EUV/far UV missions. Mirror coatings consisting of an EUV mirror under bare aluminum may be the best hope that far-UV and EUV astrophysicists have for future observations of dim sources. With clever planning of the optical path, EUV observations might be made simultaneously with IR-optical-UV. Though large diffraction-limited mirrors for the EUV are currently not feasible, they may become more possible with time, allowing the improved resolution which short wavelengths can provide[17]. Work is progressing to achieve suitable smoothness[18].

It is anticipated that a future space observatory will be located far enough from Earth that oxygen from the atmosphere will be negligible. Researchers have estimated that under such circumstances contamination of the mirror surface from its environment will be negligibly slow. Even in near-Earth orbit, a wakeshield could protect the mirrors for decades[19]. On the other hand, there are reports of carbon-containing materials building up on aluminum mirrors[20]. Thus, the stability of pristine bare aluminum surfaces in UHV requires examination.

There are two ways to get bare aluminum in space, coating at the point of use or removing a protective coating there. Both require final mirror processing in space at the point where the observatory is stationed. We report here on several

studies relative to protective barrier layers on aluminum applied prior to earth-atmosphere exposure that can be expected to be cleanly removed at the point of use in outer space leaving pristine, bare aluminum, front-surface mirrors. Since telescope mirrors are already recoated in situ in some terrestrial observatories, e.g., the Large Binocular Telescope, Mount Graham, Arizona (http://abell.as.arizona.edu/~lbtsci/scihome.html) processing at point-of-use may not be too high a hurdle[21].

In the next section, we report on some designs for these "aluminum on extreme ultraviolet (EUV) mirrors". We will then discuss issues relative to vacuum-removable barrier layers. There are three basic methods that need discussion: 1. Dry chemical processing, 2. Physical processing, and 3. Mechanical coating removal. The first is particularly promising. A form of dry chemical processing using a low-energy, low-mass plasma or atomic beam could be suitable for etching the protective barriers while leaving the underlying aluminum unaffected. This approach has not been proposed previously nor researched. It will be discussed in Section 3. The low-mass and energy of the projectile hydrogen atoms means that there is the expectation that the aluminum will not be roughened. We report a project (Section 3) on the etching of barrier polymers with hydrogen. This includes a vacuum depositable polymer, parylene. One advantage of hydrogen is that the products that form are gases like methane and other simple hydrocarbons in the case of a carbon-based coating, or silane for an amorphous silicon barrier. These all have very high vapor pressures and should immediately leave without condensing on, or in any way contaminating, the mirror or other components of the observatory. It is important to note that the traditional reactions based on oxygen or fluorides are not suitable for such a process. These are expected to etch/oxidize the mirror as well as the coating.

Physical removal. Removable Volatile Aluminum Protection (REVAP): Re-evaporation at the point-of-use of an oxygen-barrier layer on Al was proposed by Burton[22]. We have recently examined Burton's original approach and in Section 5 report our studies of REVAP.

Mechanical coating removal. This has not been discussed in print for a space-based mirrors. Essentially one would contemplate a thick protective coating like Opticlean™ that is applied in vacuum at point of fabrication and is removed in space, perhaps, by a robot on a boom. The boom would allow it to travel directly above, but without resting on the surface of the mirror. Imagine "Wall·E" on a track running along a removable curved beam above the mirror. Our group has experience working with studying the removal of Opticlean from aluminum mirrors[23], we will not report on this approach at the present, however. Similarly, such a robot on a boom geometry would provide the atomic hydrogen necessary to remove the barrier layer in the dry-chemical approach.

In section 4 we will consider the use of spectroscopic ellipsometry (SE) as a relatively easy-to-use tool which enables the study the oxidation of thin-film Al layers under barrier layers.

2. COMPUTATION OF DUAL-BAND AND EXTENDED-BAND MIRRORS

As is evident in Figure 1, using bare aluminum should extend the utility of Al mirrors 3-4 eV into the far UV past the current limit of ~11-12eV. This is the point for which the reflectance of current fluoride-coated mirrors[5] drops below 60%. We have devised ways to provide Al mirrors with significant reflectance (>40%) another few eV into the EUV further. This will be done by depositing the right combination and thicknesses of materials on the substrate prior to depositing the aluminum. In brief, this is the idea of the 'extended-range' and 'dual-band' mirrors. The range of a front-surface, bare aluminum mirror's reflectance can be extended further into the VUV/EUV range by placing it on top of an EUV multilayer mirror designed for this purpose. This is the reasoning: At energies above aluminum's plasma edge (15 eV) aluminum's reflectance falls to a few percent. However, at this point thin aluminum films also becomes partially transparent. This suggests that rather than giving up on having broadband mirrors that reach above 15 eV, we could see the aluminum as a window allowing the mirror's reflectance to be determined by underlying layers, in this case a previously deposited EUV multilayer reflector designed for just this function. This could allow the composite mirror to have > 40% reflectance several eV above aluminum's plasma edge at 15 eV.

As examples of what could be done in this region we have designed several mirrors using a genetic algorithm to optimize reflectance at wavelengths shorter than 85 nm while preserving high reflectance at longer wavelengths. The various designs involve global maximization of a merit function chosen to highlight desirable features. For instance, the merit function which generated the mirror in Figure 2 maximized the average reflectance between 65 and 110 nm with a weight of 1.0 and maximizing the reflectance at 30.4 nm with a weight of 0.5. In figure 3 the merit function optimizes a 10-layer mirror near 200 Å, that is, on the transparent side of the aluminum L edge. It consists of alternating aluminum and molybdenum and/or ruthenium layers, as shown in Table 1. Even though the program was free to choose whatever it wanted from a list of materials, for this short wavelength, it devised approximately the kind of

"high index-low index stacks" that optical designers traditionally use, though the thicknesses are not precisely periodic.

The mirror in Figure 4 shows an “extended aluminum mirror” optimized for 45° from normal. The merit function employed maximized the average reflectance between 80 and 110 nm while extending the region below 80 nm as far as possible with a reflectance equal to at least 50%.

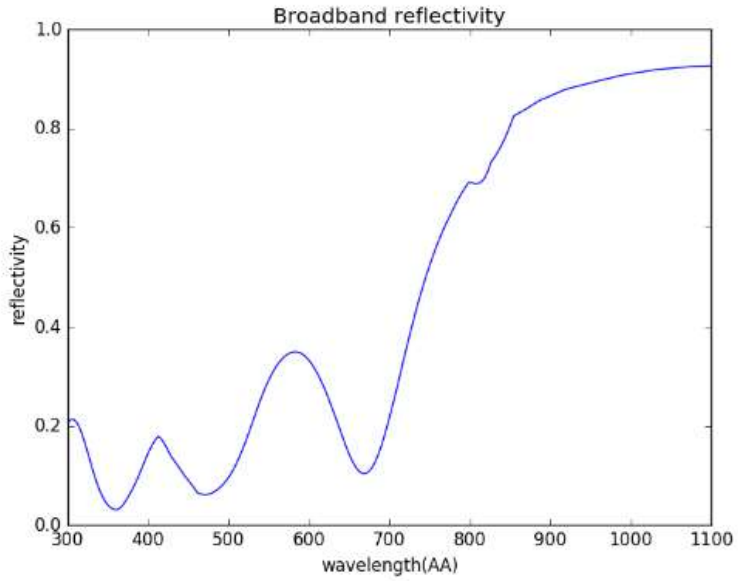


Figure 2. Calculated reflectance of a multilayer mirror with a thin aluminum cap at normal incidence as a function of wavelength in Å.

The possible materials for the mirrors were chosen from a list of 59 materials for which we had index of refraction data in this wavelength range and confidence we could use to create layers in a thin film mirror. In some cases, data was sparse over the given range and we needed to interpolate between widely spaced data points.

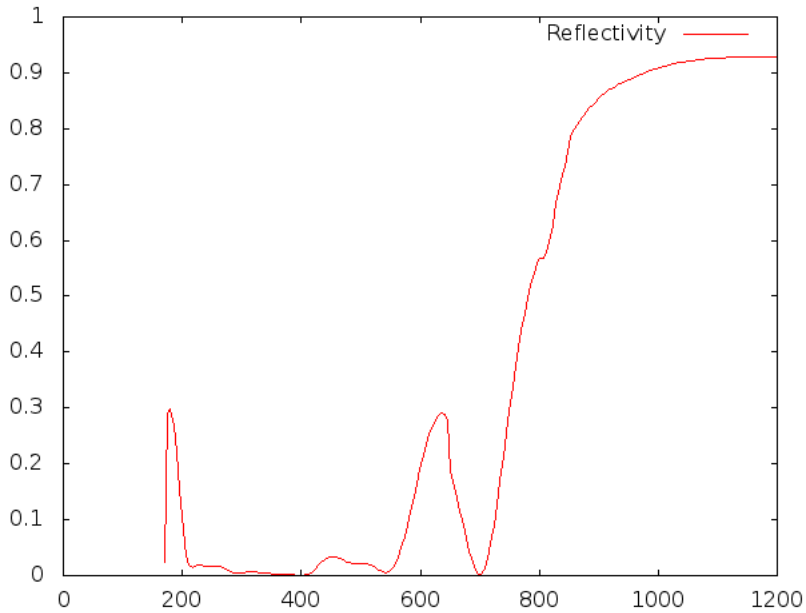


Figure 3**.** Calculated reflectance of a 10-layer multilayer mirror designed to have high 190Å-reflectance at normal incidence as function wavelength in Å. Its layer thicknesses are shown in table 1.

Table 1. 10-layer mirror show in figure 3

Layer	Material	Thickness
10	Al	59.5 nm
9	Mo	3.93 nm
8	Al	5.33 nm
7	Mo	4.32 nm
6	Al	5.17 nm
5	Mo	4.53 nm
4	Al	5.59 nm
3	Ru	4.48 nm
2	Al	5.0 nm
1	Ru	5.4 nm
Substrate	SiC	

The merit function is maximized by first selecting a large population of trial mirrors which various choices of materials and thicknesses. In order to find a good global minimum, populations of around 100,000 were typical for large mirrors. The selected merit function was computed for each of these trial mirrors and they were ranked from best to worst. From each generation, a succeeding generation was found by first selecting the top 40 mirrors from the current generation. A gradient-based local optimizer was used to fine tune the thicknesses of each of these samples. Then they were included in the pool of mirrors for the next generation. The rest of the mirrors in subsequent generations were composed of hybrid mirrors from the previous generation. The mirrors to construct the hybrid were picked with a probability proportional to the rank of their merit function. After hybridization, a small fraction of the mirrors was allow to mutate to add additional genetic variation. The process of computing merit functions and constructing subsequent generations was repeated until the merit functions of the best solutions stopped changing much between generations.

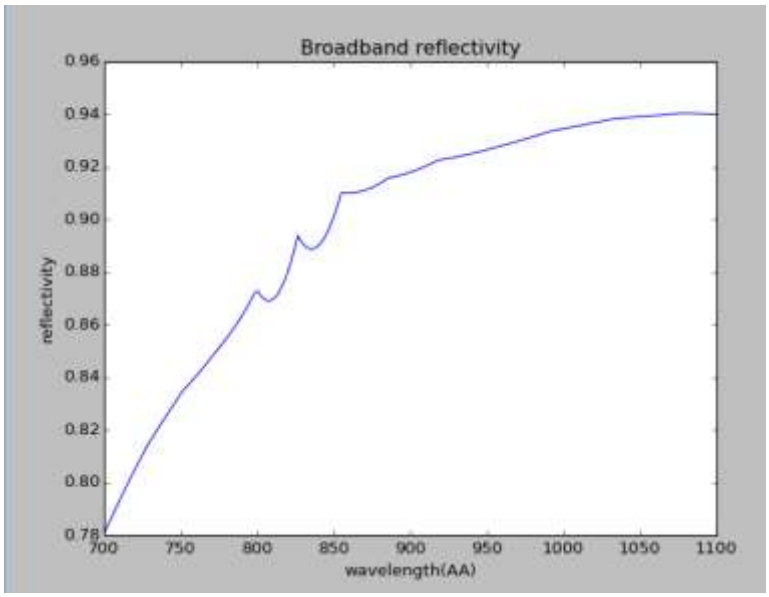


Figure 4: Calculated reflectance for a six-layer multilayer. Structure between 800 to 850 Å is due to interpolation differences between different data sets of material optical properties.

The genetic algorithm proved ideal for this design problem because the parameter space was extremely large and had a lot of local minima. Furthermore, some mirror characteristics such as the material choice for each layer could not be incorporated into the same kind of gradient-based algorithms we used for final optimization of layer thicknesses.

3. THIN-FILM ORGANIC MATERIALS ETCHED BY HYDROGEN PLASMAS

The object of dry etching is to remove all or part of an overcoat. Commonly, such dry etching is done with the aid of plasmas which break up gases form more reactive etchants. For polymer coatings on silicon devices these etching gases often include oxygen[24]. Fluorides, such as CF_4, are also used for amorphous carbon and polymer films. Aluminum is commonly used as an etch stop in many processes. Unfortunately, the aluminum surface is left altered, though the depth of the reaction is unknown. The use of fluoride containing gases could leave the mirror surface coated with fluoride.

Thus, dry etching has not been extensively researched for aluminum. However, Larruquert and Keska-Kuha, in 2008 investigated the use of inert-gas ion beams to sputter clean an aluminum oxide-coated aluminum surface[25]. They noted that the process roughened the surface. There is a lesser-known etchant that is more appropriate. This species is atomic hydrogen. The low-mass (1u) of projectile, hydrogen atoms, means that there is a good possibility that conditions can be found where the surface of the aluminum will not be roughened. Indeed, it has been reported that hydrogen slowly etches semiconductors and leaves the surface of semiconductors atomically clean[26].

We report on the etching of barrier polymers with hydrogen. Coatings containing group IV semiconductors such as, amorphous-silicon, amorphous silicon carbide, amorphous carbon or even some polymers (some polymers are highly impermeable to gases) are our focus. We believe that the reagent that can most gently remove the barrier will be atomic hydrogen formed by an RF plasma or hotwire[27]. Atomic hydrogen is known to readily attack silicon- and carbon-containing layers, forming volatile hydrides. One advantage of hydrogen with group-4 elements is that the products that form are gases like methane and other simple hydrocarbons in the case of a carbon-based coating, or silane for an amorphous silicon barrier. These all have high vapor pressures and in a vacuum should immediately leave, without condensing on, or in any way contaminating, the mirror or other components of the observatory. It can be anticipated that aluminum will be relatively unetched since alanes (aluminum-hydrogen compounds) are relative unstable and do not readily form[28]. An Al surface is likely an "etch stop" for atomic hydrogen. However, this must be tested.

We also note that traditional fluoride-coated mirrors should not be altered by atomic hydrogen. It should not etch them much since the metal fluorides are quite stable. Thus, some polymer barrier layers on aluminum mirrors may be appropriate for providing additional protection for fluoride-coated aluminum mirrors.

In our etching studies, we have examined the hydrogen etching of common microelectronic coatings such as poly-methyl methacrylate (PMMA), polyamide and parylene. The first two polymers can be deposited via solution-based spin on processes. While these may not be suitable for large Al-coated mirrors, they allowed us to examine the etch rate of polymers in hydrogen plasma. The latter, parylene, is capable of being deposited in vacuum apparatuses. Several parylene dimer precursors have been used for hermetic sealing[29,30]. Thus, it is an ideal candidate for organic barrier layers on aluminum.

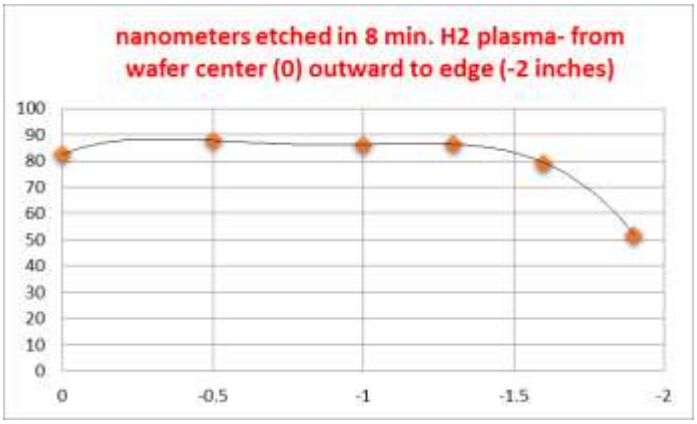


Figure 5. Depth of a etch pit of polymer on Si wafer when etched in a H2 plasma

Figure 5 shows the loss of material from the etching PMMA in a hydrogen plasma for eight minutes. A 4-inch silicon wafer with a thin film of PMMA was placed on top of a four-inch target on a Meivac magnetron sputter gun oriented in a "sputter-up" geometry in custom-built high vacuum sputter deposition system. For further details consult[31]. Instead of the usual argon sputter gas, pure hydrogen gas was introduced. The base pressure of the system was $<10^{-6}$ torr. This shows that hydrogen ions and atoms are capable of etching PMMA. Ions however are not as selective as atomic hydrogen. When the same conditions were applied to a parylene film on a silicon substrate, the film was eroded and the silicon substrate under it was attacked. See Figure 6. This experiment needs to be repeated where the substrate is aluminum coated and under conditions where atomic hydrogen is the only etchant.

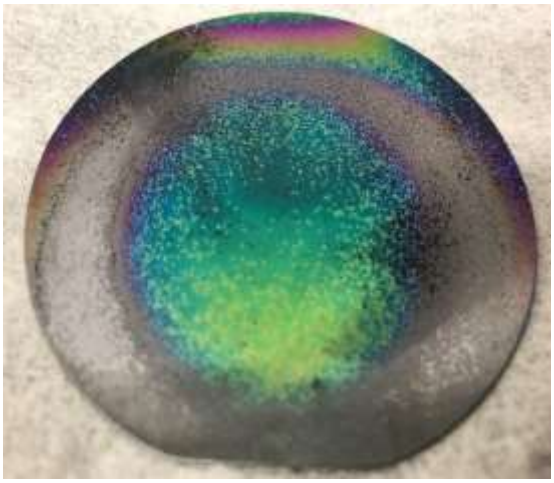


Figure 6. Lacking an Al etch stop, parylene on silicon can be overetched by H_2 plasma (gray surface are areas where Si has been removed. Areas with color are still possess coating.

4. DEVELOPMENT OF SPECTROSCOPIC ELLIPSOMETRY TO MONITOR THE OXIDATION OF THIN-FILM ALUMINUM SURFACES.

In this section, we report the development of an ex-situ tool for studying the oxidation of thin film aluminum- using variable-angle, spectroscopic ellipsometry (with microchemical analysis) as a characterization tool. The oxidation of aluminum surfaces is one of the more widely studied oxidation processes[32-53]. Aluminum thin films have played a large role in microelectronics because of their high electrical conductivity. They are also useful in providing an oxygen- and moisture-barrier in uses as diverse as food packaging and x-ray windows. And as discussed above, thin-film aluminum is useful as a broad-band mirror coating in astronomy and solar collectors reflecting from the infrared through the visible and into the ultraviolet. For astronomical and some solar energy applications the reflector is used as a 1st-surface, also termed, front-surface mirrors. There are still aspects of the oxidation that need to be better understood. We been extremely interested in developing procedures for applying modern tools that allow basic science investigation of the degradation of aluminum mirrors. Variable-angle spectroscopic ellipsometry may provide such a tool.

The technique we employed was to evaporate an ultrathin Al film (~15 to 35 nm) followed by the barrier layer (for example, MgF_2) onto the desired substrate sequentially, without breaking vacuum between the steps. This was done in a in a Denton (model DV-502 A) evaporator with two independent, resistance-heated evaporation sources. The evaporator also had a rotating sample stage, an Inficon quartz-crystal thickness monitor and a shutter activated by the thickness monitor. The over-night base pressure of the system was in the high 10^{-7} torr range. Deposition began after pump down, when the system pressure was in the mid-10^{-6} torr range. During deposition, the system pressure was observed to rise to ~$1.5x10^{-5}$ torr. This is thought to be due to water vapor's release in the chamber, as the walls are radiatively heated by the hot evaporation sources. Aluminum was usually evaporated from Al wire placed within a tungsten coil. The barrier layers were placed in standard tungsten evaporation boats. The time between the end of the evaporation of the aluminum film and the beginning of the evaporation of the overcoat was minimized to avoid oxide build up on the freshly evaporated Al and was usually less than 20 seconds. The voltage was set to be as high as practical to get evaporation rate of the l: 4-10 nm/sec. Past work has shown that high rates are conducive for producing

the purest (highly reflective) aluminum layers. The high rates are thought to limit the incorporation of oxygen into the film.

It was not our goal to replicate state-of-the-art, front-surface aluminum mirrors in every detail. Rather, we aimed at producing materials and structures as similar as possible to the relevant aspects of the mirrors. Our films are test samples for answering scientific/technological questions, such as, "what is the rate of oxidation of aluminum coatings protected by barrier layers of various compositions, thicknesses, and deposition methods?" Our samples differ from the best mirror coatings in three ways: in their thickness, in the choice of substrates and the vacuum base pressure. First, our Al films' thicknesses are mostly in the 15 to 40 nm ranges. Aluminum layers at thicknesses used in conventional mirrors would be too thick for our optical analysis-, second, in our choice of substrates-we used dielectric-coated silicon wafers (see figure 7), and third, in that they were prepared at high, not ultrahigh, vacuum. Nevertheless, we believe what we learn will be applicable to mirror-coating technology, since the oxidation of an aluminum film occurs at the top surface of the film, the bulk of the thin-film not participating in the process, and high rates produce relatively pure films. The dielectric layer on the substrate is referred to as the interference layer (IL).

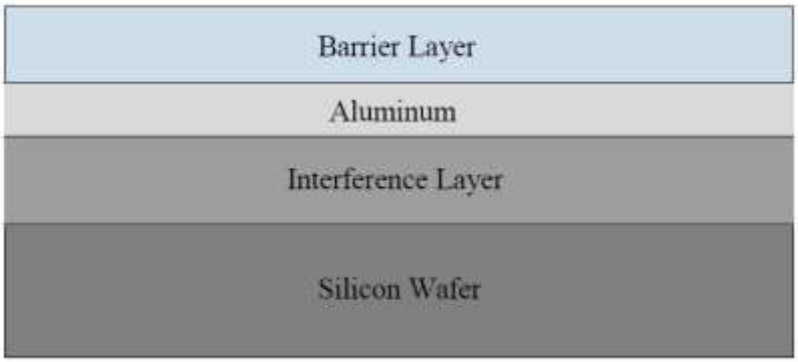


Figure 7: Diagram of the cross-sectional area of the samples grown on dielectric coated Si wafers. Ellipsometric optical models use these layers and we add interfacial layers between the top three layers. Roughness is also added on top of the barrier layer. The top 3 layers and 3 interfacial thicknesses can be fit as can the parametric optical constants.

	8 srough	0.000 nm
	7 mgf2	7.107 nm
	6 (al2o3_cl) Coupled to #0	0.513 nm
>	5 al_palik_g	34.545 nm
	4 sinonsio3	694.767 nm
	3 sio2_jaw	2.000 nm
	2 intr_jaw	0.400 nm
	1 si_jaw	10000000.000 nm

Figure 8. The layers in standard MgF2 on Al model. Thicknesses in blue indicate that a layer's thickness was fit in this trial. Other thicknesses were chosen based on prior experience (surface roughness) or for convenience (the Si substrate and its surface oxides). Layer 5 is blue because some of the parameters for aluminum's optical model were fit in this case. Their values are shown in Fig. 9.

As soon as the samples were removed from the deposition system, we characterized the samples using a John A. Woollam M2000 variable-angle, spectroscopic ellipsometer. Subsequent ellipsometric measurements were made throughout the following weeks and months. The substrates consisted of a layer of 100 to 2000 nm of dielectric, usually a CVD Si_3N_4 or SiO_2, on a piece of silicon cleaved from a polished test wafer. A 100 nm dielectric film on silicon exhibits interference fringes in reflected intensity as wavelengths are scanned from near IR through near UV wavelengths or as angle of incident light is changed[54]. The position of the fringes and their amplitude are shifted by the addition of films above the dielectric layer. For example, the absorption in the overlayer will dampen the magnitude of the fringes. The value of this for determining optical constants and thicknesses is discussed below.

To best detect and quantify the small changes in thickness of the alumina layer, it was important to make measurements of as many as possible of the layers separately and parameterize their optical constants. The indices of the Si_3N_4 interference layer (IL) were determined by measuring the coated silicon wafer. This was generally done an uncoated portion of the substrate near the sample. MgF_2 thin films were deposited and their indices measured. These well match literature values for randomly oriented MgF_2. The indices were fit using a parametric model. A Cauchy model was adequate from low energies to near the band gap of Si_3N_4 and for the whole range for MgF_2. Once the parameters for these two materials were determined their optical constants were not allowed to change while fitting the aluminum, alumina and magnesium fluoride thicknesses. A sample of evaporated aluminum on the Si_3N_4-coated substrate was also studied. Constants from that study also aided in studying the complete model.

As figures 8 and 9 show, in the example case, the nitride thickness under the Al was allowed to vary though its index was not. The blue color for thicknesses in figure 8 indicates that the thickness was fit.

	Final
MSE	3.31
Thick.4	694.767 ± 0.188
Thick.7	7.107 ± 0.169
Thick.5	34.545 ± 0.614
Thick.6	0.513 ± 0.28
En2.5	1.471 ± 0.00211
C2.5	0.44621 ± 0.00454
Eg2.5	1.1039 ± 0.0113
Amp3.5	16.278 ± 4.55
En3.5	1.0373 ± 0.0816
Br3.5	1.0965 ± 0.0412
Br1.5	0.18223 ± 0.069
Amp2.5	108.65 ± 6.99
Amp1.5	219.75 ± 68.9

Figure 9: Mean Square Error, model fitting parameters, and uncertainties for the sample discussed in figures 8 and 10. Actual uncertainties in thicknesses are somewhat larger than shown. Note that the optical constants of Al were fit in this modelling. Si_3N_4 optical constants were fit earlier. MgF_2 optical constants are from literature, but could be fit well with a Cauchy model.

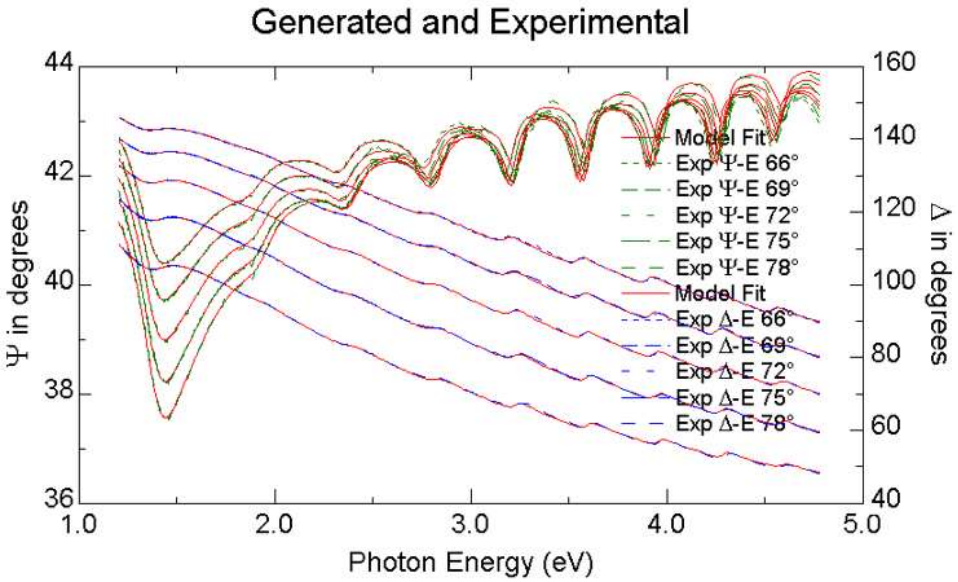


Figure 10: Ellipsometric parameter Ψ (green curves) and Δ (blue curves-scale to the right) as measured on the example sample MgF_2 (~7.5nm) on Al (~35nm) on a Si_3N_4 (~700nm) IL on Si wafer. The solid red lines are the plot of Ψ and Δ generated for the given and fit thicknesses and parameters. The angles are measured from normal incidence.

Figure 10 shows a typical set of curves measured on the example magnesium fluoride on aluminum test structure. Ellipsometric parameter Ψ (green curves) and Δ (blue curves-scale to the right) as measured on a standard sample MgF_2 (~7.5nm) on Al (~35nm) on a Si_3N_4 (~700nm) IL on Si wafer. The solid red lines are the plot of Ψ and Δ generated for the given and fit thicknesses and parameters. The angles given are from normal incidence. The comb of maxima and minima which are a prominent feature for psi are due to the interference layer. The large dip just below 1.5 eV is due to an interband transition in aluminum[55]. The position and strength of this feature depends on factors such as the crystallinity of the aluminum and measurement temperature. While adequate fits can be obtained using tabulated optical constants, adjusting parameters in a parametric model is justified given the small thickness of the aluminum layer and other depositional non-idealities. This reduces the MSE and better matches the 1.5 eV feature. Interference enhancement, as the technique is known, has been found to increase significantly the sensitivity to the absorber optical properties and thickness. The purpose of a thick dielectric layer between the absorber film and the Si substrate is to enhance the information content of multiple-angle measurements. The combination of spectroscopic ellipsometry and transmitted or reflected intensity was shown, for example, to produce a unique result for the Cr films on fused silica substrates.[56] Chemical and structural data obtained via scanning electron microscopy (SEM) coupled with energy-dispersive x-ray spectroscopy (EDS), and in some cases, atomic force microscopy, can be used to constrain which layers are present and their roughness. Finally, parametric models of the optical indices of each layer are used to produce a dramatically overdetermined system. Approximately 10,000 individual values of Δ Ψ are fit with the model possessing less than 20 adjustable parameters and usually half that number. This reduces the number of unknown model parameters and remarkably constrains layer thicknesses. Parameterization also decreases the correlation between constants while maintaining smooth, continuous, and, if desired, Kramers–Kronig consistent optical properties for the absorbing material.

We expanded the interference enhancement technique in this study by adding two layers on top of the substrate: in this example, we deposited a ~7.5nm magnesium fluoride layer on the ~35nm aluminum layer on the silicon-nitride coated silicon wafer. Continuing the example of a freshly deposited sample, we optically detected the presence, and determined the thickness of: first, the magnesium fluoride barrier layer as the top layer, second, a thin (~0.3nm) aluminum oxide film on, third, the aluminum (~35 nm) layer. As the samples aged we could see the thickness on the aluminum layer decline slightly while we saw the alumina (Al_2O_3) layer grow consistently thicker, reaching ~1.6nm in about one year.

It is noteworthy that ellipsometry can reasonably distinguish between a MgF_2 layer and an Al_2O_3 layer. They lie one above the other and there was no guarantee that the fitting program would not try to lump the two together mathematically. This success may because, though both are dielectric layers, their optical properties are distinct. MgF_2 has a low index and low dispersion, while alumina has a higher index and quite a bit of dispersion. Whatever the case, the program achieved a lower mean-square-error, MSE, for separate layers in the right order and with sensible thicknesses. Experience has shown that the "fit" thicknesses of distinct layers greater than a couple of tens of nanometers are not highly model dependent, when the mean square error is small. We observed that in our case, the deduced thicknesses were slightly dependent on the set of optical constants chosen. Over the first few hours after the sample removed from the evaporation system, the alumina layer was sufficiently thin that its apparent thickness could vary by several tenths of a nanometer depending on which set of aluminum optical constants were selected from the WVASE (John A. Woollam) database. For Al, there were three different data sets. However, after hundreds of hours it was clear that the alumina layer was increasing monotonically with time, no matter which choice was made.

Even though the program insisted on the presence of alumina in "aged" samples, distinguishing between an MgF_2 and Al_2O_3 layer, the separation wasn't perfect. It was sensible to apply a priori knowledge. For example, if we let the magnesium fluoride thickness freely vary in the model, it appeared to be increasing with time. When newly deposited, the thickness was measured to be 7.2 nm, however, this increased to 8.0 nm after more than 200 hours. We regarded this increase is unphysical; MgF_2 is not particularly hygroscopic. The film's thickness should not change. Therefore, in some of our modeling trials we set the MgF_2 thickness to be 7.1 nm, the value obtained by extrapolating to the apparent thickness to the moment of fabrication, for measurement of the sample from all times. But other values of MgF_2 thickness could be chosen. Each choice led to a different apparent thicknesses of the alumina. When we also chose 8 nm, for example, the maximum apparent alumina thickness was 0.9 nm and there was less consistency in the apparent alumina thickness over time. The trends looked unphysical. Nevertheless, since other thicknesses of MgF_2 could be chosen, the absolute thickness of the aluminum oxide could be several angstroms thicker or thinner than giving here.

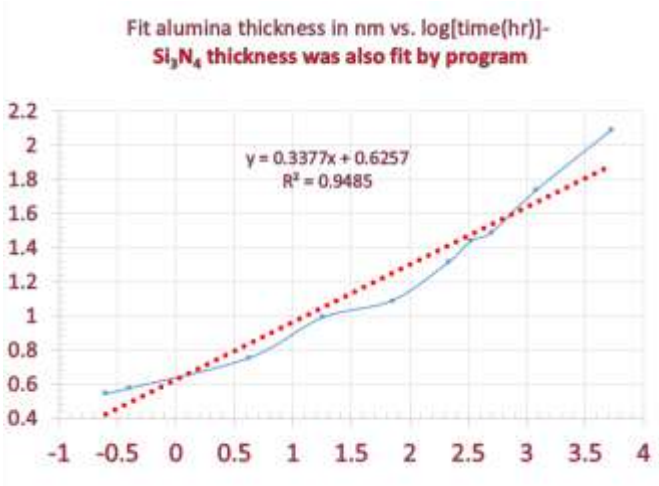


Figure 11: As determined by spectroscopic ellipsometry, the thickness of Al2O3 that has formed on 35nm Al protected by a 7.1nm MgF2 layer increases approximately linearly with the logarithm of time in hours.

The point remains that we could clearly monitor aluminum's aging and consistently compare different samples with this nondestructive, in-air and easy-to-use technique. In addition to the sample with ~7.1 nm MgF_2 reported here, we examined unprotected films (0.5 nm), and those with thicker MgF_2. We noted that the unprotected Al oxidized rather quickly and reached thicknesses of 2 nm and 5 nm after less than one hour and after 320 days, respectively.

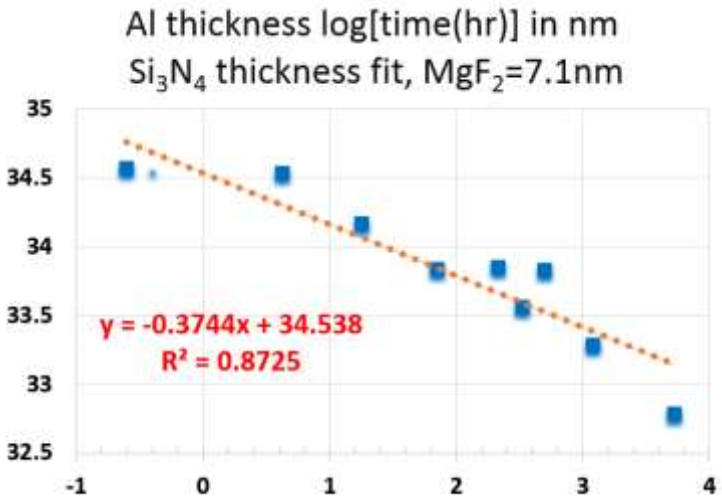


Figure 12: Aluminum thickness in ~7.1nm MgF2 protected multilayer decreases with time as determined from ellipsometric data. Over this same time the measured alumina thickness increases.

We can also say something about oxidation kinetics. For example, the alumina is seen to grow linearly with the logarithmic time, as it does for bare aluminum[43], though at a much smaller rate. The growth could be clearly measured with spectroscopic ellipsometry, though, as given by the model, the oxide coating was never much more than 2 nm. The expected complementary decline in the aluminum thickness was also noted (Fig. 12). It is heartening that we can monitor the growth of oxide and decline in aluminum thickness, ex situ, and independent of VUV reflectance measurements.

We also have some indication where the oxidation is occurring. Ellipsometry indicates that initially, at least, it is occurring on top of the aluminum film. To learn this we investigated if the model could distinguish the position of the alumina relative to the aluminum as it formed. We did this by placing a hypothetical alumina layer under the aluminum layer as well as another hypothetical aluminum oxide layer on top of the aluminum and allowed the program to

optimize the thickness of both layers. It invariably chose the hypothetical underlayer's thickness to be 0 while showing the presence of a reasonable amount of aluminum oxide layer on top of the aluminum. A next logical step would be to make VUV reflectance measurements in conjunction with our ellipsometry work.

5. REVAP: EXPERIMENTAL WORK AND DISCUSSION

5.1 REVAP

One proposed method to keep the Al reflector from oxidizing, is termed Removable Volatile Aluminum Protection (REVAP)[22]. Burton proposed using a volatile metal (i.e. metals with significantly lower vapor pressures than Al) as a barrier layer between Al and atmosphere. This barrier layer would be applied in the deposition system immediately after the Al deposition then be removed by direct application of heat in outer space. This protective layer must meet certain qualifications. Potential barrier layers must: 1. not interact with or degrade Al, but coated uniformly, 2. have low vapor pressure at low temperatures, and 3. have high vapor pressure at moderately higher temperatures.

Two candidates that may fit these parameters are cadmium and zinc. Cd forms no compounds or alloys with Al and Burton investigating Zn concluded that Zn did not interfere with the Al in the visible or near UV[4]. The relative calculated vapor pressures at 293 K of Al, Cd, and Zn are 1.7 $x10^{-49}$, 1.1 $x10^{-11}$, and 7.4 $x10^{-15}$ torr respectively, and 3.7 $x10^{-27}$, 3.7 $x10^{-4}$, and 4. 6 $x10^{-6}$ torr at 473 K. The vapor pressure of Cd and Zn are seen to differ from Al by many orders-of-magnitude. At either temperature indicated, there is no risk in vaporizing Al in the re-evaporation process. Whether the metals coat aluminum well is one of the purposes of our study.

5.2 Concerns with the REVAP approach

Some questions concerning removal of the barrier coating in space include. Where do the evaporated atoms go? They likely will condense on the first cool surface they contact. Not all the places where atoms condense are benign. Will heating the mirror distort it? Will the observatory have sufficient means of heating it? Will all have the atoms leave? If the metals oxide is comparatively non-volatile, what then?

There also coating concerns. Will layer be sufficiently robust to allow handling and aligning? The coating be smooth enough to act as a mirror to allow alignment? Will it effectively block oxygen's access to the aluminum? That is, act as a barrier layer?

Despite these concerns we investigated the REVAP process to increase our understanding[57].

5.3 Cadmium, zinc and aluminum thin-film deposition

Dielectric layers on silicon substrates were the substrates we chose for this experiment, since interference enhancement can expedite spectroscopic ellipsometric characterization via of the deposited barrier layer/aluminum film combination as discussed in section 4. Both silicon nitride and silicon dioxide dielectric layers were used in the study of cadmium barrier layers, whereas only SiO_2 layers were used in the case of zinc barriers. In the case of the zinc, two different layers thicknesses of SiO_2 were employed ~150 nm and ~1000 nm. Samples were also deposited on quartz microscope slides during the same deposition as the samples on silicon wafers. The purpose was to see if films could be characterized via-back-surface spectroscopic ellipsometry. The surface roughness that made it impossible to analyze other films is not seen when viewed from the back side. However, this proved not to be useful at the present.

Films were deposited in the Denton evaporator using the techniques described in section 4 for MgF_2 on aluminum samples. Aluminum layer thicknesses for all the cadmium samples were nominally 3 nm. Three different nominal thicknesses of cadmium barrier layers were studied, namely 5, 7.5 and 10 nm. In the case of zinc, the nominal aluminum thickness was 10 nm and two thicknesses of zinc were examined, nominal 10 nm and a nominal 20 nm.

5.4 Characterization and results

In addition to spectroscopic ellipsometric characterization some of the deposited films were studied by SEM/EDS. Any oxygen seen in the spectra for films deposited on silicon nitride was due to oxidation of the deposited cadmium and/or the aluminum films since the nitride didn't have measurable oxygen content. EDS showed no evidence of oxidation in the Cd/Al films on Si_3N_4. Atomic percentage as given by EDS (10 kVA accelerating voltage) are Si 39.4, N 57.1, Cd 2.6, Al 0.87 and O 0. Note that N/Si = 1.45, which is close to 1.33. The nominal thickness of cadmium (aluminum) are 10 nm (3 nm) respectively. The SEM derived ratio is 3.0. We conclude that cadmium may have been effective in preventing oxidation or, more likely, that the extent of oxidation cannot be detected using EDS.

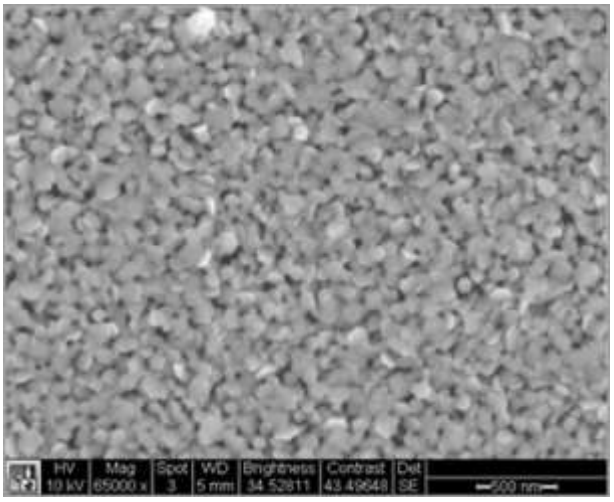


Figure 13: SEM image of Sample 11. Zn (nominal 20nm) on Al (nominal 3nm). Note hexagonal Zn platelets at random angles produces a rough, highly porous surface.

Figure 13 and 14 show SEM photos of the surfaces. These micrographs indicate that the films are very rough and are likely porous. The films have grown by island growth. It appears there are spaces between the crystal islands. It is not surprising that the films have grown this way the deposition temperature is close to the melting point of the cadmium and zinc. Under such conditions, high adatom surface mobility can lead to island formation and drastic agglomeration when and surface energetics do not favor surface wetting. That is, it is apparent that there is less attraction between the barrier layer atoms (cadmium or zinc) to the surface atoms (aluminum) then for the barrier layer atoms to each other. Such agglomeration can be expected to make zinc and cadmium poor barriers for blocking aluminum surface oxidation.

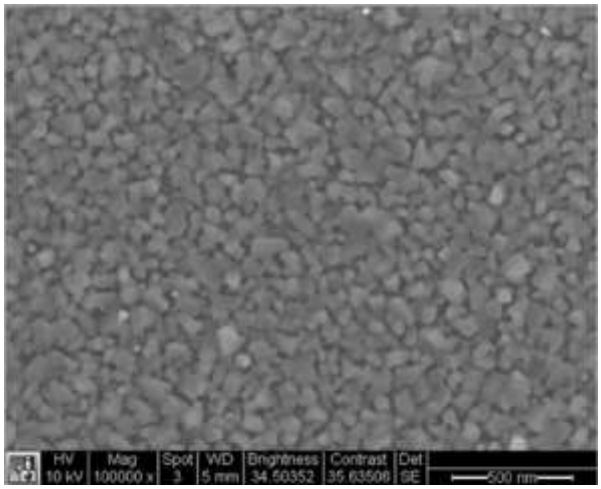


Figure 14: SEM image of Sample 5. Cd (nominal 10nm) on Al (nominal 3nm) shows agglomerated, highly faceted crystalline surface. Note the gaps between grains.

Spectroscopic ellipsometry indicated that changes were happening in the films as time elapsed. See figure 15. However, we could not build an optical model that fit the data to show which layer was changing and by how much. The samples were visibly hazy. The fraction of light reflected specularly was greatly reduced.

We show instead a plot of one ellipsometric parameter, Ψ, as a function of photon energy. In figure 15 each line corresponds to a different time after deposition and exposure to air. Can be seen that most of the changes occur in the first few minutes after the sample has been exposed to air. After that very little change is noted.

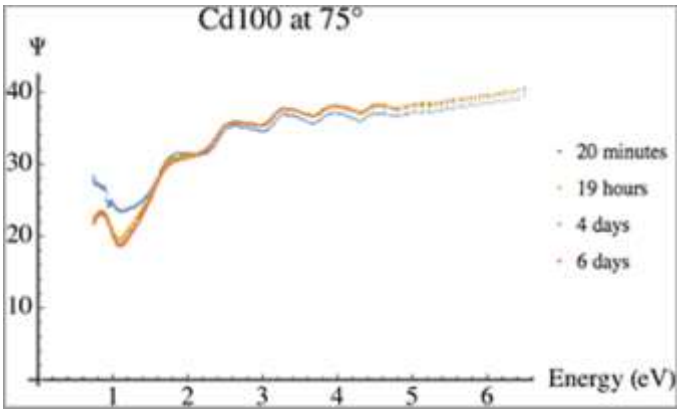


Figure 15: plots of the ellipsometric parameter, Ψ, as a function of photon energy. Each line corresponds to a different time after deposition and exposure to air.

5.5 Re-evaporation of the barrier layers

For completeness, we examined the vacuum "re-evaporation" of the cadmium and zinc overlayers from aluminum. Once the samples were characterized with ellipsometry, SEM, and EDS, pieces were broken from them and placed in the Denton for thermal re-evaporation. Of the collection of samples 'reevaporated', only Sample 5, the cadmium on aluminum film, was characterized post-REVAP. Sample 5 is the same one shown in the previous figures.



Figure 16: A picture of Sample 5 (Cd on Al) after re-evaporation. Point A, B, and C indicate locations on the sample that were to be measured with EDS to determine how much Cd was removed by the re-evaporation process.

Figure 16 shows Sample 5 post-REVAP. By visual inspection, it is evident that the barrier layer of Cd in Sample 5 was unevenly removed, as suggested previously. The green sections are the SiO_2/Si substrate, and provide a strong contrast to differentiate visually between surface compositions. The grey film is the Cd barrier layer, having been removed unevenly from the Al during re-evaporation. Point A (3.7), B (3.8), and C (3.9) indicate a gradient of removal effectiveness, from most effective (Point A) to least effective (Point C). Figure 17 shows the SEM images of point C from Sample 5. At Point A, the atomic percent composition as measured by EDS indicated approximately 60% removal of Cd. Point B had approximately 36% Cd removed and Point C had approximately 28% removed. These percentages indicate that the Cd barrier layer was not evenly removed by thermal re-evaporation–at least not the way we heated it. This figure shows evidence of "ripening". That is, some of the crystals have grown larger at the expense of smaller crystals. This will produce light scattering. A mirror coated in such a way would not be suitable for optical applications until every bit of the barrier were removed. This is one more reason why the REVAP method is probably not desirable.

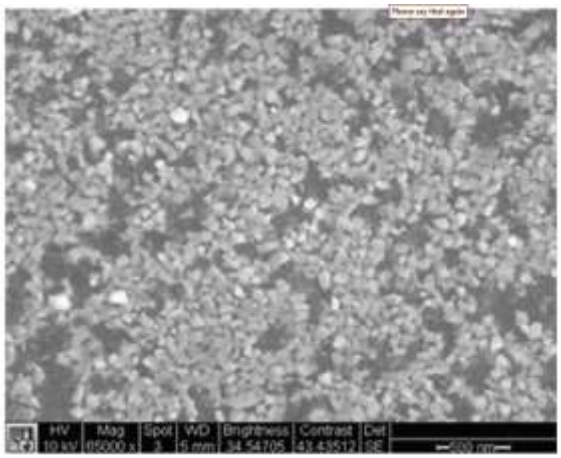


Figure 17: Sample 5 post-REVAP, point C. The atomic composition of Cd removed from the sample was 28%. Crystals have grown and become more distinct. Large open areas are evident.

6. SUMMARY AND CONCLUSIONS: LIMITATIONS AND RECOMMENDATIONS

One aim has been to devise and test several robust barrier coatings that can be readily applied in the vacuum chamber where the Al film is deposited, protecting it from surface contamination/ oxidation for minutes to days or longer while it is transported to another laboratory or to another deposition or characterization system. We have shown that hydrogen plasmas can remove organic layers, including the vacuum depositable material, parylene. This is one step along the way towards producing barriers can be removed without allowing either mirror oxidation or system contamination. However, the work has not progressed to the point that either organic or inorganic films have been shown to be barriers, nor has the behavior of aluminum mirror surfaces or fluoride barrier layers in the presence of atomic hydrogen or hydrogen plasmas been studied. Stable, robust well-characterized barriers could be useful right now, e.g., in expediting studies aimed at raising the TRL of the advanced fluoride-coatings for Al mirrors required for various applications. The REVAP technique was also investigated but exhibits several substantial problems for protecting front surface aluminum mirrors. Further information on the REVAP experiments are available online.[57]

In addition, we have used a genetic algorithm and optical constants available through the IMD program and from individual researchers to determine several promising multilayers composed of bare aluminum over the appropriate EUV mirrors. (See Fig. 2-4.) Test multilayers need to be fabricated and their reflectance in the extreme ultraviolet needs to be majored. These should have all layers but the top (bare) aluminum mirror deposited.

We have devised, used, and, here, explicated a new technique for measuring progress of aluminum oxidation under barrier layers. This technique involves the use of variable-angle, spectroscopic ellipsometry. We have begun applying it to amorphous-silicon barrier layers and aluminum-fluoride containing layers. We have also measured the EUV optical properties of the aluminum fluoride in the extreme ultraviolet. The spectroscopic ellipsometry with interference layer enhancement shows great promise in providing basic science information about potential space mirror coatings and may allow more sophisticated lifetime testing. It could be adopted for other projects.

7. ACKNOWLEDGMENTS

Michael J. Greenburg, Spencer B. Perry, and Stephanie M. Thomas, were supported by a National Science Foundation REU/RET 1461219 and 1431454. Margaret Miles was partially supported by a grant from the Utah NASA space grant consortium, project NASA Grant NNX15AI24H which also supported the project generally. We thankfully acknowledge John E. Ellsworth, Department of Physics and Astronomy, Brigham Young University for his help with vacuum systems. We acknowledge W. Scott Daniel, Department of Physics and Astronomy, BYU for his assistance in producing and maintaining stable plasmas. We profited from discussions with Prof. Matthew Linford, Department of Chemistry and Biochemistry, Brigham Young University and ellipsometric measurements were performed in his laboratory. Scanning electron microscope measurements were made part with help from Paul Minson, Brigham Young University. Atomic force microscopy measurements were made with help from Berg Dodson. Measurements. We

thank Dr. Igor Olegovich Usov, Engineered Materials Group, Materials Science and Technology Division, Los Alamos National Laboratory for providing us parylene films on silicon wafers.

8. REFERENCES

[1] Bolcar, M. R., Balasubramanian, K., Crooke, J., Feinberg, L., Quijada, M., Rauscher, B. J., Redding, D., Rioux, N., Shaklan, S., Stahl, H. P., Stahle, C. M. and Thronson, H., "Technology gap assessment for a future large-aperture ultraviolet-optical-infrared space telescope," Journal of Astronomical Telescopes, Instruments, and Systems 2, 0412091-9 (2016).

[2] Hass, G., Hunter, W. R. and Tousey, R., "Reflectance of Evaporated Aluminum in the Vacuum Ultraviolet," Optical Society of America, 46(12), 1009-1012 (1956).

[3] Gervais, F., "Aluminum Oxide (Al203)," in [The Handbook of Optical Constants II], Academic Press, 761-75 (1991).

[4] Wilbrandt, S., Stenzel, O., Nakamura, H. and Wulff-Molde, D.,"Protected and enhanced aluminum mirrors for the VUV," Applied Optics 53, 125-130 (2013).

[5] Balasubramanian, K., Hennessy, J., Raouf, N., Nikzaa, S., Ayala, M., Shaklan, S., Scowen, P., Hoyo, J. D. and Quijada, M., "Aluminum Mirror Coatings for UVOIR Telescope Optics including the Far UV," Proc. SPIE 9602, 96020I (2015).

[6] Moore, C. S., Hennessy, J., Kersgaard, E. and Jewell, A. D., "Current progress in the characterization of atomic layer deposited AlF3 for future astronomical ultraviolet mirror coatings," Proc. SPIE 9601, 96010X (2015).

[7] Moore, C. S., Hennessy, J., Jewell, A. D., Nikzad, S. and France, K., "Recent developments and results of new ultraviolet reflective mirror coatings," Proc. SPIE 9144, 91444H (2014).

[8] Hennessy, J., Balasubramanian, K., Moore, C. S., Jewell, A. D., Nikzad, S., France, K. and Quijada, M., "Performance and prospects of far ultraviolet aluminum mirrors protected by atomic layer deposition," Journal of Astronomical Telescopes Instruments and Systems 2(4), 041206-041206 (2016).

[9] Sembach, K., Calzetti, D., Ebbets, D., Green, J., Greenhouse, M., Heap, S., Hillenbrand, L., Kaiser, M., Lazio, J. and Marcum, P., "Cosmic Origins Program Analysis Group Report to Paul Hertz Regarding Large Mission Concepts to Study for 2020 Decadal Survey," (2015). https://cor.gsfc.nasa.gov/docs/COPAG_Flagship_Response_final.pdf

[10] Hall, D. T., Gladstone, G. R., Moos, H. W., Bagenal, F., Clarke, J. T., Feldman, P. D., Mcgrath, M. A., Schneider, N. M., Shemansky, D. E., Strobel, D. F. and Waite, J. H., "Extreme-Ultraviolet Explorer Satellite Observation of Jupiter Io Plasma Torus," Astrophysical Journal 426, 51-54 (1994).

[11] Scowen, P. A., Perez, M. R., Neff, S. G. and Benford, D. J., "Scientific objectives for UV/visible astrophysics investigations: a summary of responses," Experimental Astronomy 1, 1, (2013). arXiv:1306.0553 [astro-ph.IM]

[12] Seely, J. and Hunter, W. R., "Thin-film interference optics for imaging the oxygen II 834-Angstrom airglow," Applied Optics 30(19), 2788-94 (1991).

[13] Sandel, B. R., Broadfoot, A. L., Chen J., Curtis, C. C., King, R. A., Stone, T. C., Hill, R. H., Sigmund, O. H. W., Raffanti, R., Allred, D. D., Turley, R. S. and Gallagher, D. L., "The Extreme Ultraviolet Imager Investigation for the IMAGE Mission," Space Science Reviews 91, 197-242 (2000).

[14] Bowyer, S., Lampton, M., Lewis, J., Wu, X., Jelinsky, P. and Malina, R. F., "The second Extreme-Ultraviolet Explorer source catalog," Astrophysical Journal Supplement Series 102, 129-160 (1996).

[15] Barstow, M. A., Casewell, S. L., Holberg, J. B. and Kowalski, M. P., "The status and future of EUV astronomy," Advances in Space Research 53, 1003-1013 (2014).

[16] Berghofer, T. W., Bowyer, S. and Korpela, E., "Extreme Ultraviolet Explorer observations of clusters of galaxies: Virgo and M87," Astrophysical Journal 535, 615-620 (2000).

[17] Salashchenko, N. N. and Chkhalo, N. I., "Diffraction-limited short-wavelength optics: Analysis, fabrication, and application," Journal of Surface Investigation-X-Ray Synchrotron and Neutron Techniques 6, 464-472 (2012).

[18] Chkhalo, N. I., Churin, S. A., Mikhaylenko, M. S., Pestov, A. E., Polkovnikov, V. N., Salashchenko, N. N. and Zorina, M. V., "Ion-beam polishing of fused silica substrates for imaging soft x-ray and extreme ultraviolet optics," Applied Optics 55, 1249-1256 (2016).

[19] Larruquert, J. I., Mendez, J. I. and Aznhrez, J. A., "Degradation of far ultraviolet reflectance of aluminum films exposed to atomic oxygen. In-orbit coating application exposed to atomic oxygen," Optics Communications 124, 208-215 (1996).

[20] Krijger, J. M., Snel, R., Harten, G. v., Rietjens, J. H. H. and Aben, I., "Mirror contamination in space I: mirror modelling," Atmospheric Measurement Techniques 7, 3387-3398 (2014).

[21] Atwood, B., Pappalardo, D., O'Brien, T., Hill, J. M., Mason, J., Belville, R., Steinbrecher, D., Brewer, D., Teiga, E., Sabol, B., Howard, J. and Miglietta, L.,"The Aluminizing System for the 8.4 Meter Diameter LBT Primary Mirrors," Proc. SPIE 6273, 62730T (2006).
[22] Burton, W. M., "Removable volatile protective coatings for aluminized mirrors used in far-ultraviolet space astronomy," J. Phys. D: Appl. Phys., 16, L129-L132 (1983).
[23] Robinson, R., Sandberg, R., Allred, D., Jackson, A., Johnson, J., Evans, W. T., A. Baker, D. T., Adamson K. and Jacquier, A., "Removing Surface Contaminants from Silicon Wafers to Facilitate EUV Optical Characterization," in [47th Annual Technical Conf.], Soc. of Vacuum Coaters, Albuquerque, 368-376 (2004).
[24] Hartney, M. A., Hess, D. W. and Soane, D. S., "Oxygen Plasma-Etching for Resist Stripping and Multilayer Lithography," Journal of Vacuum Science & Technology B 7, 1-13 (1989).
[25] Larruquert, J. I. and Keska-Kuha, R. "Removal of a protective coating on aluminum by ion etching for high reflectance in the far UV," Applied Optics 47(29), 5253-59 (2008).
[26] Chang, R. P. H., Chang, C. C. and Darack, S., "Hydrogen Plasma-Etching of Semiconductors and Their Oxides," Journal of Vacuum Science & Technology 20, 45-50 (1982).
[27] Soer, W. A., van Herpen, M. M. J. W., Jak, M. J. J., Gawlitza, P., Braun, S., Salashchenko, N. N., Chkhalo, N. I. and Banine, V. Y., "Atomic-hydrogen cleaning of Sn from Mo/Si and DLC/Si extreme ultraviolet multilayer mirrors," Journal of Micro-Nanolithography Mems and Moems 11 (2), 021118-0211184 (2012).
[28] Siegel, B., "The Reaction between Aluminum and Atomic Hydrogen," Journal of the American Chemical Society 82, 1535-1537 (1960).
[29] Kahouli, A., Sylvestre, A. and Laithier, J.-F., "Performance improvements of the hydrophobic and the dielectric properties of parylene C," Journal of Applied Physics 114, 1541111-1541117 (2013).
[30] Madakasira, P., Inoue, K., Ulbricht, R., Lee, S. B., Zhou, M., Ferraris, J. P. and Zakhidov, A. A., "Multilayer encapsulation of plastic photovoltaic devices," Synthetic Metals 155, 332-335 (2005).
[31] He, H., Andersson, D. A., Allred, D. D. and Rector, K. D., "Determination of the Insulation Gap of Uranium Oxides by Spectroscopic Ellipsometry and Density Functional Theory," Journal of Physical Chemistry C 117, 16540-16551 (2013).
[32] Kotenev, V. A., "Combining ellipsometry and electron microscopy for the identification of the initial stages of aluminum oxidation. I. Methodical aspect," Protection of Metals 36, 366-374 (2000).
[33] Kotenev, V. A., "Combining ellipsometry and electron microscopy for identifying the initial stages of aluminum oxidation. II. Ellipsometry," Protection of Metals 36, 409-418 (2000).
[34] Kotenev, V. A., "Combining ellipsometry and electron microscopy when identifying the initial stages of aluminum oxidation. III. Laser probe and electron microscopy," Protection of Metals 39, 415-423 (2003).
[35] Kruger, W. H. and Pollack, S. R., "Initial Oxidation of Aluminum Thin-Films at Room-Temperature," Surface Science 30, 263-279 (1972).
[36] Barna, P. B., Bodo, Z., Gergely, G., Szigethy, D., Adam, J. and Jakab P., "Electron-Microscopic and Ellipsometric Studies on Oxidized Aluminum Layers," Vacuum 33, 93-97 (1983).
[37] Reichel, F., Jeurgens, L. P. H. and Mittemeijer, E. J., "The effect of substrate orientation on the kinetics of ultra-thin oxide-film growth on Al single crystals," Acta Materialia 56, 2897-2907 (2008).
[38] Barna, P. B., Bodo, Z., Gergely, G., Croce, P., Adam, J., Jakab, P., "Ellipsometric and X-Ray Specular Reflection Studies on Naturally Grown Overlayers on Aluminum Thin-Films," Thin Solid Films 120, 249-256 (1984).
[39] Bujor, M., Larson L. A., and Poppa, H., "A Study of the Initial Oxidation of Evaporated Thin-Films of Aluminum by AES, ELS, AND ESD," Journal of Vacuum Science & Technology 20, 392-395 (1982).
[40] Barna, P. B., Bodo, Z., Gergely G. and Adam J., "Spectral Ellipsometric TEM and Electron Spectroscope," Vacuum 36, 465-469 (1986).
[41] Brune, H., Wintterlin, J., Trost, J., Etrl, G., Wiecher J. and Behm, RJ, "Interaction of Oxygen with Al(111) Studied by Scanning-Tunnelling-Microscopy," Journal of Chemical Physics 99, 2128-2148 (1993).
[42] Cabera, N. and NF, M. "Theory of the oxidation of metals," Reports on Progress in Physics 12, 163-184 (1948).
[43] Fehlner, F. P., "Low-Temperature Oxidation of Metals and Semiconductors," Journal of the Electrochemical Society 131, 1645-1652 (1984).
[44] Batra I. P., and Kleinman, L., "Chemisorption of Oxygen on Aluminum Surfaces," Journal of Electron Spectroscopy and Related Phenomena 33, 175-241 (1984).
[45] Martin, M. and Fromm, E., "Kinetics of Aluminum Film Oxidation Measured by a Modified Quartz-Crystal Microbalance," Thin Solid Films 236, 199-203 (1993).
[46] Martin, M., Mader, W. and Fromm, E., "Oxidation of Iron, Aluminum and Titanium Films in the Temperature-Range 50-200-Degrees-C," Thin Solid Films 250, 61-66 (1994).

[47] Grimblot, J. and Eldridge, J. M., "Interaction of Al Films with O-2 at Low-Pressures 1," Journal of the Electrochemical Society 129, 2366-2368 (1982).
[48] Grimblot, J. and Eldridge, J. M., "Oxidation of Al Films 2," Journal of the Electrochemical Society 129, 2369-2372 (1982).
[49] Khan, J. M. and Makowiecki, D. M., "Investigation of Room-Temperature Oxidation of Aluminum Thin-Films by Scanning High-Energy Electron Diffraction," Surface Science 77, L155-L161 (1978).
[50] Jeurgens, L. P. H., Sloof, W. G., Tichelaar F. D. and Mittemeijer, E. J., "Growth kinetics and mechanisms of aluminum-oxide films formed by thermal oxidation of aluminum," Journal of Applied Physics 92, 1649-1656 (2002).
[51] Vanderkolk, G. J. and Verkerk, M. J., "Microstructural Studies of the Growth of Aluminum Films with Water Contamination," Journal of Applied Physics 59, 4062-4067 (1986).
[52] Verkerk, M. J. and Vanderkolk, G. J., "Effects of Oxygen on the Growth of Vapor-Deposited Aluminum Films," Journal of Vacuum Science & Technology A-Vacuum Surfaces and Films 4, 3101-3105 (1986).
[53] Vinodh, M. S., Jeurgens, L. P. H. and Mittemeijer, E. J., "Real-time, in situ spectroscopic ellipsometry for analysis of the kinetics of ultrathin oxide-film growth on Mg-Al alloys," Journal of Applied Physics 100, 044903 (2006).
[54] Drevillon, B., "Spectroscopic Ellipsometry of Ultrathin Films - From UV to IR," Thin Solid Films 163, 157-166 (1988).
[55] Smith, D. Y., Shiles, E. and Inokuti, M., "The Optical Properties of Metallic Aluminum," in [The Handbook of Optical Constants of Solids 1], Academic Press, 369-406 (1985).
[56] Hilfiker, J. N., Singh, N., Tiwald, T., Convey, D., Smith, S. M. , Baker, J. H. and Tompkins, H. G., "Survey of methods to characterize thin absorbing films with Spectroscopic Ellipsometry," Thin Solid Films 516, 7979-7989 (2008).
[57] Thomas, S. M., "Preventing Oxidation of Aluminum Mirrors with Cadmium and Zinc Barriers," Senior thesis of the Department of Physics and Astronomy, Brigham Young University, 2017, https://www.physics.byu.edu/docs/thesis/773 (1 July 2017).